J. Physiol. (1986), **376**, *pp.* 63–83
With 8 text-figures
Printed in Great Britain

ASYMMETRIC CHARGE MOVEMENT IN CONTRACTING MUSCLE FIBRES IN THE RABBIT

BY G. D. LAMB

From the Department of Physiology, John Curtin School of Medical Research, Australian National University, G.P.O. Box 334, Canberra ACT 2601, Australia

(*Received 17 June 1985*)

SUMMARY

1. The Vaseline-gap technique was used to record asymmetric charge movement in small segments of muscle fibres from the white sternomastoid or the soleus muscle of the rabbit. At 22 °C, non-linear ionic currents (Na^+, K^+, Cl^-, Ca^{2+}) were virtually eliminated for potential steps to 0 mV or below by specific blocking agents or ion substitution.

2. A Boltzmann fit of charge movement (Q) *vs.* potential (V) produced the mean values $Q_{max} = 15{\cdot}2$ nC/μF, $V = -26{\cdot}8$ mV and $k = 15{\cdot}3$ mV for twenty-three sternomastoid fibres, and 4·8 nC/μF, −32 mV and 13·7 mV for seven soleus fibres. Q_{max} for the sternomastoid fibres was similar to that for other fast-twitch fibres when normalized by surface area rather than capacitance.

3. Using a 55 ms step, the mean threshold potential (V_{th}) for contraction in twenty-eight fibres was −25·9 (±2·9) mV (±S.E. of mean), and the mean amount of charge moved (q_{th}) at the threshold potential was 8·5 (±0·4) nC/μF.

4. In some contracting fibres, a component of charge movement was observed which was analogous to q_γ in amphibian muscle in its time course and potential dependence.

5. Addition of 80 mM-sucrose to the external solution increased the speed of both the asymmetric charge movement and the charging of the linear capacitance of each fibre. The effect was reversible. A clear relation between the time course of these two parameters was established, and this strongly indicated that the majority of the asymmetric charge was located in the transverse tubular system or beyond. Moreover, it was shown that at 22 °C nearly all asymmetric charge moved in less than 0·5 ms after depolarization of the T-system.

6. Sucrose in the external solution affected the Q *vs.* V relation, steepening the curve and shifting it to more negative potentials, as well as slightly increasing Q_{max}. The actions of sucrose strongly suggest that it effectively dilates and/or shortens the transverse tubular system, probably by osmotic effects.

INTRODUCTION

It is known that depolarization of the transverse tubular system is normally necessary to evoke contractions in a muscle, but the succeeding steps leading to calcium release from the sarcoplasmic reticulum (s.r.) are poorly understood. When

most ionic currents in skeletal muscle have been blocked and the linear capacitive currents removed, depolarizations from the normal resting potential have been shown to produce small membrane currrents which have been proposed to underlie or reflect the process leading to Ca^{2+} release (Schneider & Chandler, 1973; Adrian & Almers, 1976; Chandler, Rakowski & Schneider, 1976*a*, *b*; Kovacs, Rios & Schneider, 1979; Hollingworth & Marshall, 1981; Dulhunty & Gage, 1983).

For amphibia, the charge movement in response to depolarizing steps from the resting potential has been subdivided into two components, q_β and q_γ (Adrian & Peres, 1979; Huang, 1982; Hui, 1983). The larger component, q_β, can be observed even when depolarizing steps from the resting potential are small and, with larger depolarizations, the q_γ component appears as a distinct 'hump' on the q_β component. From observations of charge movement in fibres able to contract (Horowicz & Schneider, 1981*a*, *b*; Huang, 1981), it was found that the time and potential at which q_γ appears is closely related to the twitch threshold. However, it is not clear whether q_γ causes, is a consequence of, or is unrelated to Ca^{2+} release and contraction.

In previous investigations of mammalian charge movement, micro-electrodes have been used for recording potentials and passing current, and muscle contraction has been blocked with hypertonic sucrose solutions (Hollingworth & Marshall, 1981; Simon & Beam, 1985*a*, *b*) or tetracaine (Dulhunty & Gage, 1983, 1985). One of the aims of this study was to examine charge movement in mammalian fibres that are able to contract, and to investigate the effects of sucrose and tetracaine. This was achieved by using the Vaseline-gap method (Hille & Campbell, 1976). The fibre was made sufficiently slack between the Vaseline seals so that it was possible to record charge movement during contraction with minimal or no electrical artifact and no damage to the fibre. This enabled the quantification of the charge moved at the contraction threshold, which had not previously been examined in mammalian muscle. It was also possible to investigate whether a q_γ component could be identified near the contraction threshold. A further advantage of the Vaseline-gap technique is that it gives access to both internal and external environments of the fibre, making it possible to reduce ionic currents much more than in micro-electrode experiments, especially at higher temperatures where such currents substantially affect measurement of charge movement (Simon & Beam, 1985*a*, *b*).

The location of asymmetric charge movement, which is crucial for any putative role it might have in excitation–contraction coupling, is disputed. Experiments examining the time course of charge movement (Simon & Beam, 1985*a*, *b*) or the effect of detubulating the fibres, at least partially (Chandler *et al.* 1976*b*; Dulhunty, Gage & Barry, 1981; Campbell & Hahin, 1983) have led to the conclusion that charge movement resides in the tubular system (or beyond, in the adjacent s.r. membrane). In contrast, Adrian & Huang (1984*b*), who examined the dependence of q_β and q_γ on fibre diameter, concluded that only the smaller component, q_γ, was located in the transverse tubular system.

It is shown in this paper that the charging of linear capacitance and asymmetric charge movement occur more rapidly in solutions made hypertonic with sucrose than in isotonic solutions. The differences in the results of some previous studies can be accounted for by this finding. Furthermore, the relation between the movement of the linear and asymmetric charge strongly indicates that, in mammalian muscle, the

majority of charge movement is located in the transverse tubular system (or beyond). The pharmacological subdivision of charge movement in mammalian muscle, and the basis of the components, are considered in the following paper (Lamb, 1986). Some of these results have been reported briefly elsewhere (Lamb, 1985*a*, *b*).

METHODS

Dissection and fibre mounting

The sternomastoid or the soleus muscle was dissected free from rabbits killed by a bolt shot through the hind brain. The muscle was pinned out in a shallow dish lined with Sylgard (Dow Corning, Midland, U.S.A.), and in the case of the sternomastoid muscle, the bundles of white muscle

TABLE 1. Solutions used (mM)

Dissecting solution (pH 7·3)

	Na^+	K^+	Ca^{2+}	Mg^{2+}	Cl^-	glucose
D	140	5	2·5	1	152	11

Internal solutions (pH 7·0)

	Na^+	Cs^+	Mg^{2+}	Glutamate	ATP
I_1	156	0	0	155	0·5
I_2	154	0	1	155	0·5
I_3	1	153	1	155	0·5

External solutions* (pH 7·3)

	TEA†	Mg^{2+}	Ca^{2+}	Br^-	SO_4^{2-}	2,4D‡	sucrose
E_1	150	8	0·2	150	8·2	2·5	0
E_2	150	8	0·2	150	8·2	2·5	80

All solutions also contained 2 mM-TES§ buffer and, with the exception of solution E_2, were adjusted to an osmolality of 290 mosM by the addition of the principal salt. Cs^+ solutions also contained 0·1 mM-EDTA to chelate heavy metals.

* Both external solutions contained 10^{-6} M-tetrodotoxin, pH adjusted with NaOH, H_2SO_4.

† Tetraethylammonium.

‡ 2,4 dichlorophenoxyacetic acid.

§ *N*-tris[hydroxymethyl]methyl-2-aminoethanesulphonic acid.

fibres, which run down both sides of the whole muscle, were cut away from the red muscle bundle. The muscle bundles, bathed in a Krebs solution (D, Table 1), remained healthy for more than 8 h. A section (3–4 mm) of a single white sternomastoid or soleus fibre was isolated and transferred to the perspex 'Vaseline-gap' bath. The Vaseline-gap bath (Hille & Campbell, 1976) consisted of four distinct compartments, which were normally separated by threads of a special Vaseline (Glisseal, Borer Chemie AG, Switzerland) (Fig. 1), although they were initially covered and joined by a surplus of the internal solution (I_1, I_2 or I_3, Table 1). When in position, three seals of Glisseal were made around the fibre. Additional segments of Glisseal were placed on both sides close to the fibre in both the A and B pools to ensure that, when the solution level was dropped in the whole bath, a substantial layer of fluid still bathed the fibre; this decreased any problems with series resistance. The width of the A pool was decreased by sliding a movable section of the bath which supported the EA seal, to ensure that the fibre was initially slack in the A pool in the event of contractions. The length of fibre in the E, A, B and C pools was typically 200, 300, 100 and 200 μm respectively, and the seals were 200 μm wide. The total length and average diameter of the fibre in the A pool were measured under a microscope for use in calculations involving fibre surface area. The fibre

ends in the E and C pools were cut again longitudinally and the fibre was left for at least 30 min. All experiments were conducted at 22 °C.

Voltage clamp and electrical recordings

The voltage-clamp method used was based on that of Hille & Campbell (1976). Five $Ag^+/AgCl$ half-cells were connected to the gap pools by glass bridges filled with 1 M-KCl in agar. (In later experiments the bridges in the end pools were filled with the internal solution in agar to eliminate a small outward K^+ current which affected some records.) Junction potential differences were eliminated by previous equilibration of the half-cells, and any small remaining differences were noted before experiments. Changes in junction potentials, produced by subsequent solution substitutions in pool A, were measured relative to 3 M-KCl micro-electrodes, and later compensated for. Separate current-passing and potential-sensing electrodes, A_1 and A_2, were positioned on opposite sides of the fibre in the A pool to minimize series resistance artifacts. The voltage clamp held point D (Fig. 1) at ground potential, and the solution in the A pool was replaced with either solution E_1 or solution E_2. The command wave form was generated by a DEC PDP 11/23 microcomputer and blunted by a low-pass filter with 0·1 ms time constant. The actual transmembrane potential was ascertained in six cases by inserting a 3 M-KCl micro-electrode into the fibre in the A pool close to the AB seal and measuring the potential difference relative to another micro-electrode; the transmembrane potential closely resembled the command voltage and had less than a 2 mV offset in every case. The total current passed by Amplifier 2 was monitored by the potential difference across a 200 kΩ feed-back resistor. A two-time constant capacitive wave form, generated using the voltage command signal, was subtracted from the current record in order roughly to cancel linear elements, when necessary. Both the subtracted current record and the record of the potential of the A_2 electrode, V_m, were filtered by a four pole Bessel filter with a corner frequency of 1 or 4 kHz and sampled and stored by the microcomputer at 5 or 10 kHz respectively.

Pulse protocol and analysis procedure

The membrane potential of the fibre (the negative of the A_2 potential) was clamped at −90 mV and subjected to a 55 ms 'control' step of −20 or +10 mV relative to the holding potential, followed 70 ms later by a depolarizing 'test' step, also 55 ms long (Fig. 2). For each test step, the sequence of two pulses was reproduced between one and four times, 2 s apart, and the average of the resultant records was stored for both the voltage and current channels. Remaining linear capacitive and ionic currents were removed in later analysis by scaling and subtracting the 'synthetized' control current (see Horowicz & Schneider, 1981*a*) from the test current. The amount of asymmetric charge moved was calculated by fitting and extrapolating base lines to the data and integrating the transient current (Chandler *et al.* 1976*a*; Horowicz & Schneider, 1981*a*). Charge movement was expressed relative to the linear capacitance of the fibre, which was determined using a 10 mV depolarizing step from the holding potential.

Effects of finite seal resistance

The Vaseline seals were of high resistance, probably 5 MΩ or more, but their effect on both dynamic and steady state current measurements should be considered. Any leak through the AB seal will not affect either the current or the voltage record, and so can be neglected. Fig. 1 shows the leak resistance through the EA seal, R_1, the longitudinal resistance of the fibre, R_i (~ 200 kΩ), and the impedance of the membrane in the A pool subdivided into a pure resistive component, R_m, and the remainder, Z_m. At any time t, the total current $I_t(t)$ is the sum of the leak current $I_l(t)$ and the membrane current $I_m(t)$, the latter of which can be broken into (a) the current through R_m, $I_r(t)$ which is proportional to $V_m(t)$, and (b) the capacitive current, $I_c(t)$, which flows through Z_m and declines to zero at long times if $V_m(t)$ reaches a steady state. As point D is a virtual ground, the potential in pool A is $V_m(t)$ and in pool E is:

$$V_e(t) = -I_m(t)\,R_i = -(I_r(t)+I_c(t))\,R_i. \tag{1}$$

The potential difference between the A and E pools is $V_m(t)-V_e(t)$, and $V_m(t) = I_r(t)\,R_m$, thus the leakage current is:

$$I_l(t) = \frac{V_m(t)-V_e(t)}{R_l} = V_m(t)\frac{(R_i+R_m)}{R_m R_l} + I_c(t)\frac{R_i}{R_l}. \tag{2}$$

Thus both $I_l(t)$ and the recorded current, $I_t(t)$ can be broken into two parts, one purely resistive and proportional to $V_m(t)$, and the other related to the capacitive current $I_c(t)$

$$I_t(t) = V_m(t)\frac{(R_l+R_i+R_m)}{R_m R_l} + I_c(t)\frac{(R_l+R_i)}{R_l}. \tag{3}$$

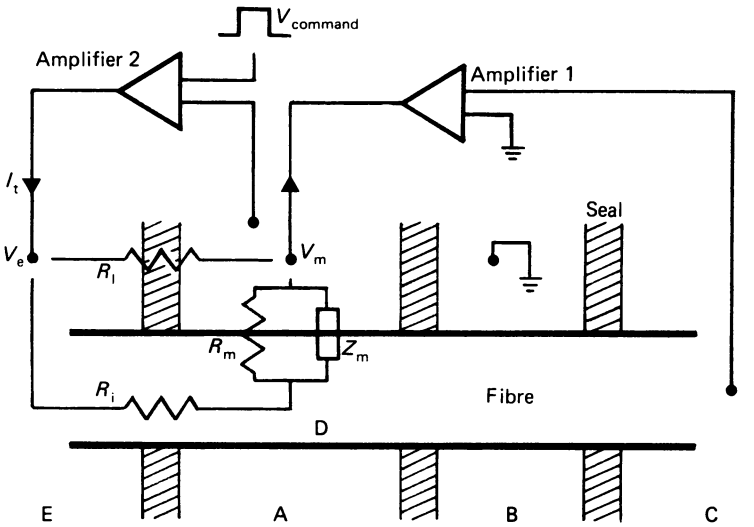

Fig. 1. Diagram of a cut muscle fibre embedded in three Vaseline seals, shown with a simplified clamp circuit. The pools of fluid separated by the Vaseline are conventionally denoted as E, A, B and C, and point D is clamped at ground potential. The dark circles represent $Ag^+/AgCl$ half-cells and agar bridges connecting the circuit to the pools. One electrode in the A pool passes current and the other monitors potential. The ohmic resistances R_l, R_i and R_m, and the capacitive impedance Z_m are described in the text together with the corresponding currents and potential differences.

To determine the linear and non-linear capacitive membrane currents, $I_c(t)$, it is necessary to remove the resistive current from the total, and this can be achieved by determining the value $(R_l+R_i+R_m)/(R_m R_l)$ from $V_m(\infty)/I_t(\infty)$ and then subtracting a suitably scaled version of the voltage record, $V_m(t)$ from the current record, $I_t(t)$ in a manner analogous of that of Schneider & Chandler (1976). The remaining current record, $I_{ceff}(t)$ given by

$$I_{ceff}(t) = I_c(t)\frac{(R_l+R_i)}{R_l}, \tag{4}$$

can be related to $I_c(t)$ only if R_l and R_i are known. However, using $I_{ceff}(t)$ instead of $I_c(t)$ in calculations of fibre capacitance will cause only a small error ($< 7\,\%$) when good seals are achieved ($R_l > 3$ MΩ) and a short, well cut, length of fibre connects the A and E pools ($R_i < 200$ kΩ). In any case, (a) the observed capacitive current will be linearly related to the true current, and (b) calculations of asymmetric charge movement, which are expressed as the ratio of the observed non-linear and linear capacitive currents, will not be affected by the error.

A lower limit to the leak resistance, R_l, can be obtained from the total resistance, R_t, of the current paths through the fibre and the Vaseline, remembering that V_e and V_m are of opposite polarity:

$$R_l > R_t = \frac{V_m(\infty)-V_e(\infty)}{I_t(\infty)} > \frac{V_m(\infty)}{I_t(\infty)}. \tag{5}$$

The mean value of $\frac{V_m(\infty)}{I_t(\infty)}$ in forty-eight fibres recorded in this study was 2·7 MΩ, and so the leak resistance R_l must have been considerably larger than this.

RESULTS

Cable properties

Cable properties were calculated for white sternomastoid and soleus fibres from twenty rabbits using the estimated surface area obtained by visual measurements. An estimate of the total resistance, R_t, to current flow through both the fibre and the EA seal (Fig. 1) was made using $V_m(\infty)/I_t(\infty)$ (eqn. (5)). The mean values shown in Table 2 were found using a solution which minimized ionic currents (solution E_1 or E_2, Table 1) and thus produced a relatively high mean membrane resistance, R_m. By having no Na^+, K^+ or Cl^- in the solution and using the chloride channel blocker, 2,4 dichlorophenoxyacetic acid, it could be assumed that the transverse tubular length constant was relatively long and thus that virtually the whole tubular capacitance was measured (Dulhunty, Carter & Hinrichsen, 1984). The values obtained here for the linear capacitance, C_m, and for the membrane resistance, R_m, in rabbit sternomastoid muscle, assuming that the leak resistance R_l was much larger than the membrane resistance, are very close to those found by a micro-electrode study which used rat sternomastoid fibres and solutions with low Cl^- or containing 2,4 dichlorophenoxyacetic acid ($C_m = 13{\cdot}5\ \mu F/cm^2$; $R_m = 2{\cdot}0\ k\Omega\ cm^2$, Dulhunty *et al.* 1984). C_m in the soleus fibres was slightly larger than that reported for rat, and R_m was about half of the value for rat (Dulhunty & Gage, 1983). The membrane resistance, R_m, was probably underestimated because of (a) underestimation of the membrane surface area by neglect of wrinkling or invaginations, and (b) appreciable leakage through the EA seal. However, as the estimate of the total resistance, R_t, is determined by both R_m and the leak resistance, R_l, the leak resistance must have been considerably greater than 2·7 MΩ (Table 2). Consequently, the error in the linear capacitance measurement (eqn. (4)) owing to leakage through the Vaseline was much less than 5 %. Some fibres did show a small increase (3–5 %) in capacitance over time which was accompanied by a substantial decrease in the estimate of R_t. It is inferred that the leak resistance through the Vaseline, R_l, had substantially decreased in such cases.

TABLE 2. Cable properties of white sternomastoid and soleus fibres in the rabbit (mean ± S.E. of mean). R_t is an estimate of the total resistance in the Vaseline-gap experiment (see text)

	n	C_m ($\mu F/cm^2$)	R_m ($k\Omega\ cm^2$)	R_t (MΩ)	Diameter (μm)
Sternomastoid	41	13·8 ± 0·6	2·2 ± 0·2	2·7 ± 0·2	77·5 ± 4·7
Soleus	7	8·0 ± 0·8	2·0 ± 0·3	2·7 ± 0·4	64·9 ± 4·8

Asymmetric charge movement

Fig. 2*C* shows records of asymmetric charge movement in which the linear capacitive and ionic currents have been removed (see Methods), but which are otherwise uncorrected (there has been no smoothing or subtraction of steady or sloping base lines). It is clear that there is at least a rough equality of the charge moved upon depolarization (ON charge) with that moved upon repolarization (OFF charge), and that there are virtually no ionic currents activated except by the largest depolarizations.

However, under certain circumstances ionic currents can affect the estimation of charge movement.

Outward current. Fig. 2*C* shows an outward current which was activated by steps to potentials greater than 0 mV. Such a current was present in every fibre, although it was usually considerably smaller than in the example shown. This current was

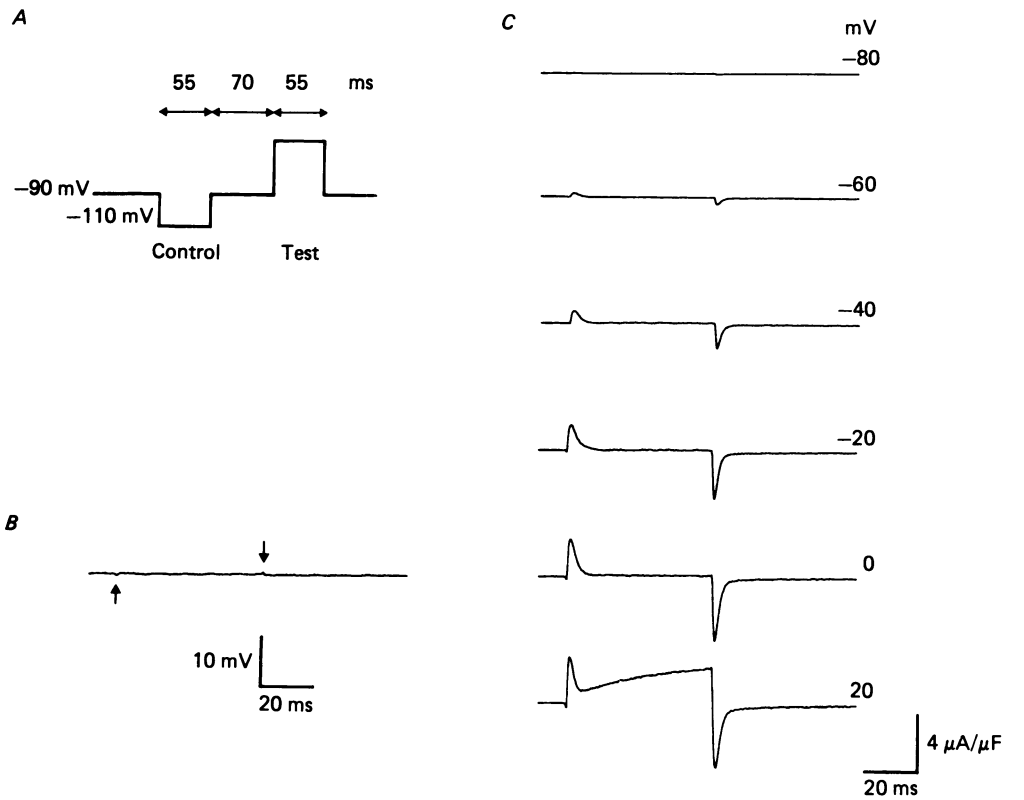

Fig. 2. Uncorrected asymmetric charge movement in a white sternomastoid fibre. The potential was held at −90 mV and then stepped as shown in *A*. The similarity of the control and test steps is illustrated in *B*, which shows the difference between a 90 mV test step and a suitably scaled copy of the −20 mV control step; the arrows indicate the start and end of the 55 ms steps. The charge movement records shown in *C* were produced when the fibre was bathed internally in a sodium glutamate solution (I_1, Table 1) and externally in a low Ca^{2+} TEABr solution (solution E_2). Each record is the average of four repetitions. C_m, 14·2 μF/cm²; R_m, 1·9 kΩ cm²; diameter, 67 μm; temperature, 22 °C.

distinctly different from the delayed potassium channel current (Adrian, Chandler & Hodgkin, 1970; Duval & Leoty, 1978), which was observed in this study when the fibre was bathed in normal Krebs solution. The delayed potassium current was usually activated near −40 mV and could be blocked, at least partially, by TEA^+ and 4 mM-4-aminopyridine, although neither blocked the current reported here. The current shown in Fig. 2 was probably not carried by either K^+ or Cl^- as neither ion was present in the internal or external bathing solutions and yet the current appeared to increase rather than diminish with successive stimuli. It was not necessary to have

Ca^{2+} in the external solution in order to produce the outward current (Fig. 3), nor was it blocked by 5 mM-Co^{2+}. However, addition of 0·2 mM-Cd^{2+} to the external solution substantially reduced this outward current in two fibres, but caused very rapid deterioration of the fibres. Thus the involvement of Ca^{2+} in this current is not clear. Regardless of the ionic basis of the outward current, the presence of an accompanying tail current might have affected the estimation of the OFF charge for steps to +20 mV or greater.

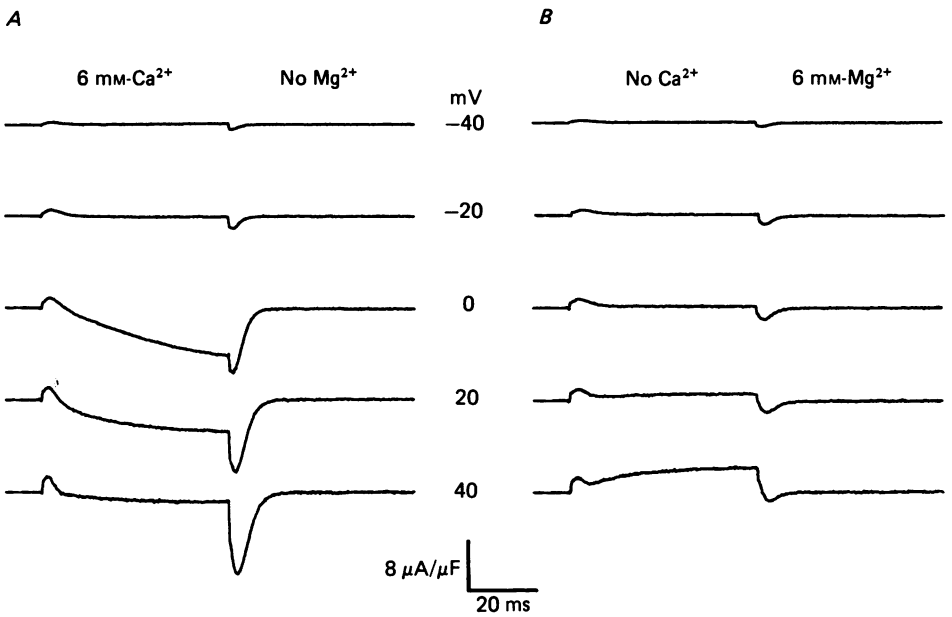

Fig. 3. Asymmetric charge movement and Ca^{2+} currents in solutions with and without external Ca^{2+}. *A*, the fibre was externally bathed in (mM): TEABr, 150; $CaSO_4$, 6; TES, 2; 2,4 dichlorophenoxyacetic acid, 2·5. *B*, the charge movement in the same fibre when the external solution was changed to one in which Mg^{2+} completely replaced Ca^{2+}, but which was otherwise identical. The inward Ca^{2+} current is clearly visible in the records of steps to 0 mV and above in *A* and is absent in *B*. The calcium tail current greatly exaggerates the OFF charge in *A*. C_m, 11·2 μF/cm²; R_m, 4·2 kΩ cm²; diameter, 62 μm.

Brief inward current. Initially, estimation of asymmetric charge movement was complicated in many fibres by the apparent presence of a small inward current which appeared to be activated by depolarizations to potentials more positive than −80 mV, and which inactivated completely between 5 and 30 ms after depolarization. Subsequent investigation revealed that, in most cases, this current was an artifact of the subtraction procedure, owing to the presence of an inward current during the hyperpolarizing control steps. Use of a synthesized control current (Horowicz & Schneider, 1981*a*) eliminated this problem. The small inward current evoked by the hyperpolarizing control step was not blocked by 10 mM-Rb^+, 10 μM-tetrodotoxin, 20 mM-Co^{2+} or 100 μM-nifedipine in the external solution, or by 150 mM-Cs^+ in the internal solution. (With the exception of nifedipine, these agents also did not affect the asymmetric charge.) A similar current was observed in rat extensor digitorum

longus (e.d.l.) and soleus muscles using the three micro-electrode voltage clamp (A. F. Dulhunty, P. W. Gage & G. D. Lamb, unpublished observations).

Calcium current. An important part of the procedure for the clear identification of charge movement was the removal of virtually all of the Ca^{2+} current. All previous experiments, both with amphibian and mammalian muscle, have used normal or elevated $[Ca^{2+}]$ in the external solution. Horowicz & Schneider (1981*a*) and Dulhunty

TABLE 3. Boltzmann parameters (mean ± S.E. of mean) giving the best fit in thirty-two white sternomastoid and seven soleus fibres

	n	Q_{max} (nC/μF)	$\overline{V}$ (mV)	k (mV)
All sternomastoid data	32	14·4 ± 0·5	−26·6 ± 0·7	14·5 ± 0·3
Sternomastoid (+10 mV control step)	9	12·6 ± 1·0	−26·1 ± 1·2	12·1 ± 0·4
Sternomastoid (−20 mV control step)	23	15·2 ± 0·6	−26·8 ± 0·9	15·3 ± 0·3
Soleus	7	4·8 ± 0·6	−32·6 ± 2·1	13·7 ± 0·9

& Gage (1983) have shown that in both types of muscle the resulting Ca^{2+} current can cause an over-estimation of the OFF charge, though this can be blocked by 20 mM-Co^{2+}. Fig. 3 shows that a large inward current was activated at 0 mV in solutions with external Ca^{2+}, and was not present when Ca^{2+} was totally replaced by Mg^{2+}. It is clear from the largest potential step in Fig. 3*A* that ionic currents can give a very misleading indication of the apparent charge movement; in this case the Ca^{2+} current was roughly equal to the outward current during the potential step but the Ca^{2+} tail current greatly exaggerated the OFF charge. In the following experiments Ca^{2+} currents were virtually eliminated by Mg^{2+} substitution, and thus there was no need for any Ca^{2+} channel blocker. A small amount of Ca^{2+} was added to the solution (0·2 mM-$CaSO_4$) to block any non-selective cation conductance of the type reported for frog muscle (Almers, McCleskey & Palade, 1984).

Charge movement vs. potential

The relation between the amount of charge moved, Q, and the membrane potential during the test step, V, was examined by fitting the data from each fibre with a Boltzmann equation:

$$Q = Q_{max}/[1+\exp(\overline{V}-V)/k], \quad (6)$$

and determining the values of (a) the maximum charge, Q_{max}, (b) the potential giving half maximum charge, $\overline{V}$ and (c) the slope factor, k, which together produced the lowest variance (Schneider & Chandler, 1973). The estimate of the OFF charge was used in the calculations as it was considered more accurate than that of the ON charge, because the OFF charge was usually faster than the ON charge and also because it was not complicated by the presence of separate subcomponents. One rabbit fibre had a maximum charge (Q_{max} = 3·0) that was considerably lower than that of all the other rabbit sternomastoid fibres, and a value of $\overline{V}$ (−34·7 mV) that was 8 mV more negative than the mean value for the other fibres, so it was not included in the average data. The mean and S.E. of mean of the Boltzmann parameters for the thirty-two remaining sternomastoid fibres and seven soleus fibres are shown in Table 3. (The value of Q_{max} in sternomastoid fibres may be slightly in error because the presence

of an outward current affected the estimation of charge movement above +20 mV. However, the rate of increase of Q dropped substantially at potentials above 0 mV, indicating that the charge was probably approaching saturation. Soleus fibres showed saturation before +20 mV.) For the sternomastoid fibres, the means of the data derived using control steps of +10 and −20 mV (relative to the holding potential) are also shown separately. The mean value of Q_{max} obtained using +10 mV control steps was significantly less ($P < 0.05$, Student's t test) than that produced using −20 mV control steps, indicating that the +10 mV control pulse itself moved an appreciable amount of charge. This amount of charge, determined using a −20 mV control pulse and a +10 mV test pulse, was typically only about 0·15–0·2 nC/μF, but its effect on Q_{max} was magnified about 14 times when the control pulse was scaled up and subtracted from the largest test pulses. Thus when a +10 mV control step was used, Q_{max} was underestimated by between 2 and 3 nC/μF (see Table 3).

The one rat e.d.l. fibre examined possessed greater charge movement (Q_{max} = 24·1 nC/μF) and a smaller linear capacitance (C_m = 8·7 μF/cm^2) than any rabbit sternomastoid fibre examined. The data from the rat fibre are very close to those found in micro-electrode studies (Dulhunty & Gage, 1983, 1985), and serve to show that the Vaseline-gap technique did not grossly underestimate the charge movement.

Contraction threshold

Eighteen (42 %) of the fibres perfused internally with Na^+ (solution I_1 or I_2) showed no visible contractions as a result of depolarizing steps, despite displaying normal charge movement and linear cable properties, and six other fibres showed a marked increase in threshold during the experiment and eventually stopped contracting. All ten fibres perfused with Cs^+ contracted when suitably depolarized. With a 55 ms pulse, the mean contraction threshold for twenty-eight fibres was −25·9 (±2·9) mV, although this included two fibres with thresholds near 0 mV. The amount of charge (q_{th}) moved by a 55 ms pulse to the threshold potential ranged between 6·0 and 12·1 nC/μF (mean, 8·5±0·4 nC/μF, n = 28). The maximum asymmetric charge that could be moved, Q_{max}, was obtained for eighteen of these fibres and had a mean of 16·3 (±0·8) nC/μF.

Components of charge movement

Records of asymmetric charge movement, especially near the contraction threshold, were closely examined to determine whether any subdivision of the charge movement could be supported on the grounds of its time course. The charge movement recorded in two typical cases is shown in Fig. 4. The charge movement recorded in a fibre which displayed a distinct second component of ON charge is illustrated in Fig. 4*A*. The top record, shown at low gain, displays the charge moved at the threshold potential (−34 mV). The other records, at higher gain, show a small hump occurring after the (truncated) main peak of the ON charge at potentials near threshold. As the fibre was subjected to greater depolarizations, the hump (q_γ) occurred at progressively earlier times until it merged with the main peak. The fibre in Fig. 4*B* twitched for every depolarization up to, or more positive than, −30 mV in the sequence shown and in two other sequences not shown. The ON charge decayed monotonically in every case. However, comparison of the records above and below threshold suggested, but did

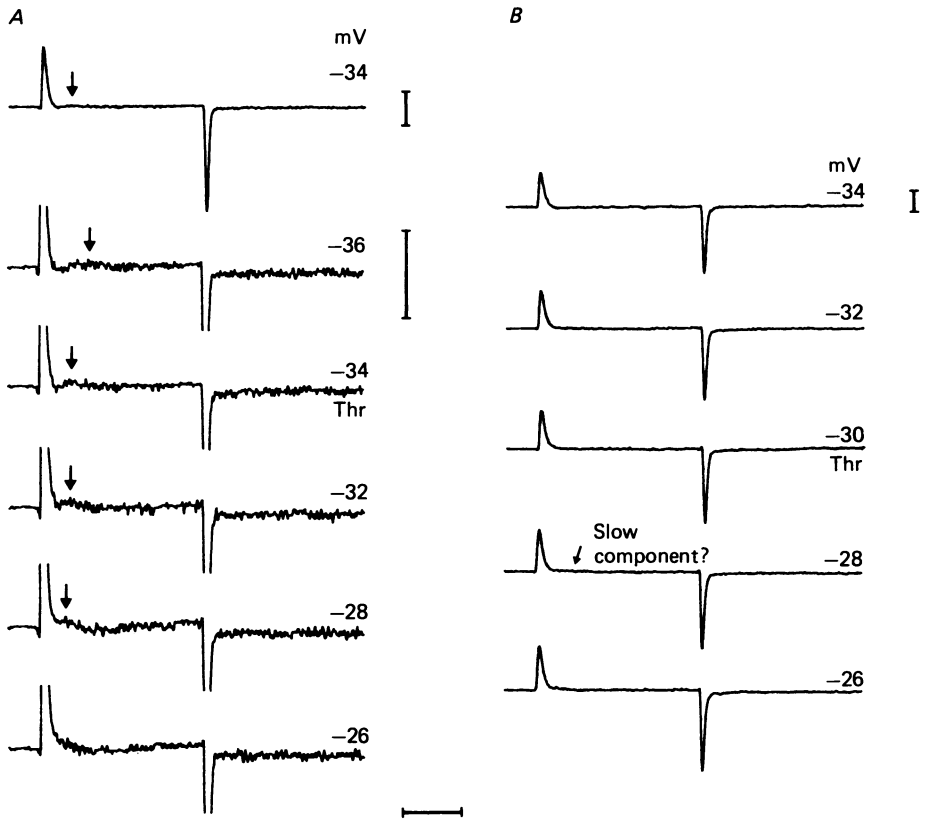

Fig. 4. Asymmetric charge movement near contraction threshold in two fibres. The records show the charge moved by a 55 ms depolarizing step to the potential indicated with each trace. *A*, one fibre displayed a very small hump immediately after the ON charge peak, at its contraction threshold (−34 mV). The hump (arrows) is seen clearly at high gain in the lower traces (truncated); it gradually merged with the majority of the ON charge for large depolarizations. *B*, the second fibre had a contraction threshold (Thr) of −30 mV, and the ON charge decayed monotonically at each potential. However, close examination of the current records evoked near the threshold suggested the possible presence of a small slow component of the ON charge. Each record is the result of a single control and test pulse pair, and has not been corrected for ionic currents. Both fibres were bathed internally with solution I_2 and externally with solution E_2. Vertical calibration bars represent 2 μA/μF, and the horizontal bar 20 ms. C_m, 12·7 μF/cm^2; R_m, 1·2 kΩ cm^2 in *A*. C_m, 14·1 μF/cm^2; R_m, 2·4 kΩ cm^2 in *B*. Temperature, 22 °C.

not convincingly prove, the existence of a small slow component of the ON charge following the main peak, for potential steps to near threshold. The presence of such an unmeasured slow component was also suggested by the fact that the ON charge peak had an area that was approximately 20 % smaller than that of the OFF charge peak at all potentials near threshold. Although a q_γ component was not identified in every contracting fibre, it was never seen in fibres which failed to contract.

An example of a large q_γ component is illustrated in Fig. 5. The traces show a clear hump following and merging with the majority of the ON charge near the threshold potential. This was the most distinct hump in charge movement seen in any fibre,

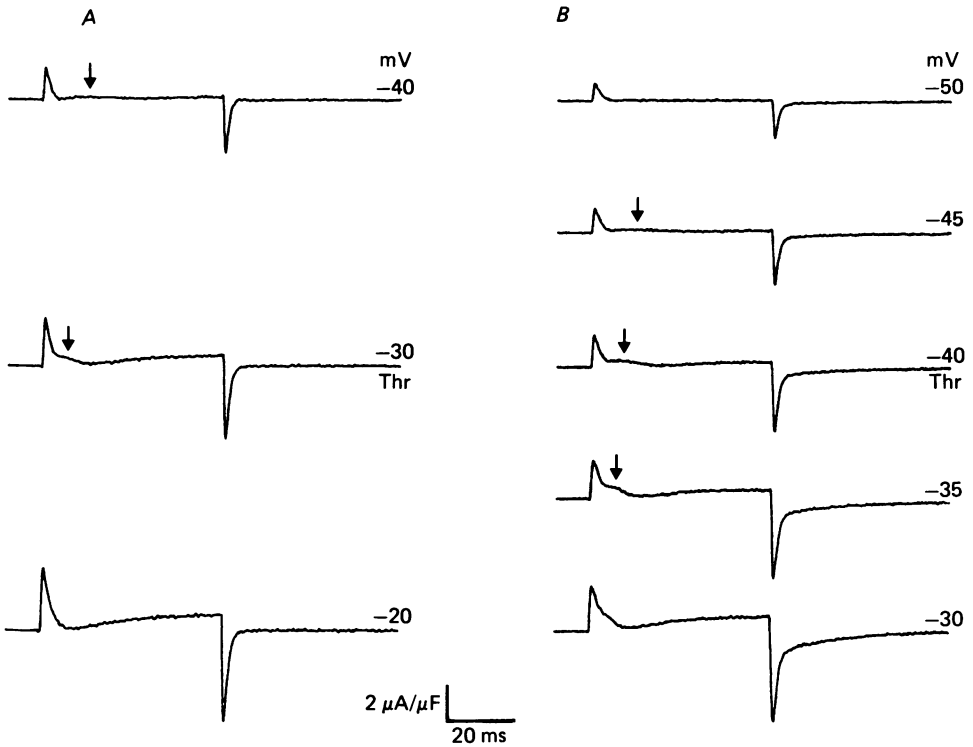

Fig. 5. Charge movement in a sternomastoid fibre displaying a distinct hump (arrows) in the ON charge. The fibre was initially examined by a sequence of depolarizing steps each 10 mV larger than the previous one; some of the resulting traces are shown in *A*. The procedure was repeated (not shown) and then repeated again using 5 mV increments (*B*) and once more using 2 mV increments (not shown). In *A* the fibre contracted at potentials of −30 mV and above, but in all subsequent examinations the contraction threshold lay between −44 and −40 mV. A clear hump during the ON charge was always observed somewhere between −45 and −30 mV. However, note that the hump occurred over a different potential range in *A* than in *B* and appeared quite similar at the potential at which contraction was first observed for each (−30 and −40 mV respectively). The outward current was probably carried by K^+ from the KCl bridges (see Methods). The OFF charge in suprathreshold records in *B* was affected by a twitch artifact which disappeared when contraction was subsequently blocked. C_m, 13·6 μF/cm²; Q_{max}, 21·1 nC/μF; diameter, 110 μm.

and was observed in each of four sequences of depolarizing steps, parts of two sequences being shown in the Figure. It is interesting to note that in Fig. 5*A* and *B* the amount and position of the charge movement hump (q_γ) appears to be more closely related to the contraction threshold than it does to the test step potential. In contrast the main peak of the ON charge (q_β) appeared to be determined by the potential. This suggests that there may not be a fixed relation between q_β and q_γ, and that q_β may not be related to the initiation of contraction. The charge movement associated with the fibre in Fig. 5 was the largest observed in any rabbit fibre (Q_{max} = 21·1 nC/μF), and the fibre itself had the largest diameter (110 μm) of any fibre studied.

Relation between the linear capacitive current and charge movement

An investigation was made of the effect of hypertonic solutions on the time course of both the linear capacitive current and asymmetric charge movement. Fig. 6 shows the records obtained from one fibre when 80 mM-sucrose was added to the external solution, and then when that solution was replaced with the original solution. Making

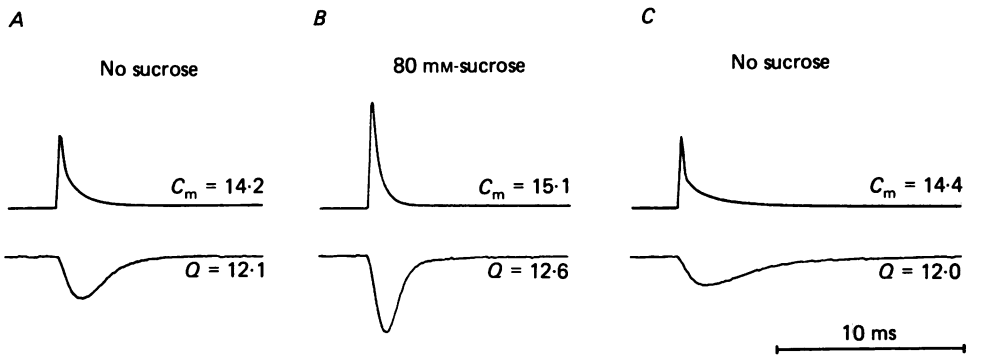

Fig. 6. Linear capacitive currents and asymmetric charge movement in a rabbit sternomastoid fibre in the presence and absence of sucrose. The linear capacitive current was produced by a +10 mV step from the holding potential, and the charge movement was produced by repolarization from 0 mV to the holding potential (OFF charge). *A*, the external solution contained no sucrose (E_1, Table 1). *B*, addition of 80 mM-sucrose clearly produced faster charging of both the linear and non-linear capacitances. *C*, replacement with the original solution slowed both wave forms. The linear capacitance (C_m) in $\mu F/cm^2$, and the amount of charge movement (Q) in $nC/\mu F$ is indicated in each case. Filter frequencies: 1 kHz (asymmetric charge), 4 kHz (linear capacitance).

the external solution hypertonic by the addition of the sucrose resulted in both faster charging of the linear capacitance and faster asymmetric charge movement, the latter being shown in the Figure by the OFF charge for a step from 0 mV back to the holding potential (a situation where the speed of the charge movement is near maximal (Simon & Beam, 1985*a*)). The measured linear capacitance and the amount of charge moved were only slightly increased. This concentration of sucrose did not noticeably affect muscle contraction. The effects were reversed when a solution without sucrose was used. Fig. 6*C* clearly shows that the linear capacitive current consisted of at least two distinct components; these are related to the charging of the surface membrane (fast component) and the transverse tubular membrane (slow component) (Hille & Campbell, 1976.) (The relation between the capacitive current components and the anatomical structures, however, is not totally straightforward as the capacitive and resistive elements are distributed.) After the addition of the sucrose the charging of the tubular capacitance was so fast that the time courses of the two components after filtering (4 kHz, see Methods) were inseparable (Fig. 6*B*). The effects detailed above were seen in all eight fibres examined both before and after the addition of sucrose. Fig. 7 illustrates the relation between the time taken to charge 90 % of the linear capacitance (including the surface capacitance) and the time taken to move 90 % of the asymmetric charge. The Figure includes data from fibres bathed in solutions with

or without sucrose. There is a significant linear correlation of the two parameters ($r = 0{\cdot}883$, $P < 0{\cdot}01$) and the intercept of the best-fit line indicates that the charge movement lagged behind the linear capacitive current by 1·2 ms. A similar relation prevailed when a smaller percentage, e.g. 60 %, of the charges was chosen as the criterion. (Fig. 7 shows some fibres in which 90 % of the asymmetric charge had moved

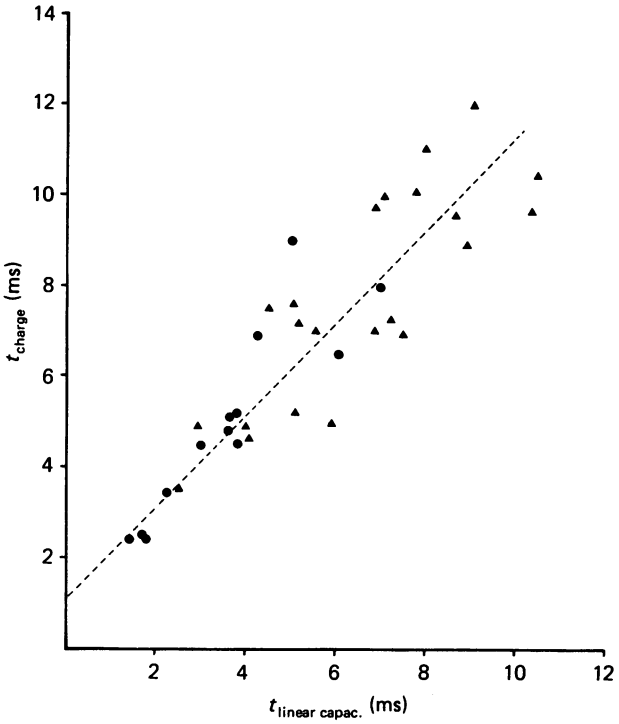

Fig. 7. Relation between the time taken to charge the linear capacitance of a fibre to 90 % of its maximum ($t_{linear\ capac.}$) and the time taken to move 90 % of the asymmetric charge (t_{charge}) for the OFF step from 0 mV to −90 mV. Data were obtained from twenty-five fibres; values recorded in solutions containing 80 mM-sucrose are shown by circles, those recorded in solutions without sucrose by triangles. The best-fit line is indicated, and it intercepts the ordinate at 1·2 ms. The difference in filtering frequency would be expected to account for about 0·75 ms of the delay between the asymmetric charge (1 kHz filter) and the linear capacitive transient (4 kHz). Thus the asymmetric charge moved within about 0·5 ms after the charging of the T-system.

before a similar proportion of the linear capacitive charge, but this is possibly due to the presence of a third, even slower, capacitive component which was observed in some fibres, and small inaccuracies involved in fitting the sloping base lines needed to identify and integrate the asymmetric charge.) The relation shown in Fig. 7 is most easily explained if the time course of the asymmetric charge movement is largely determined by the charging of the tubular system.

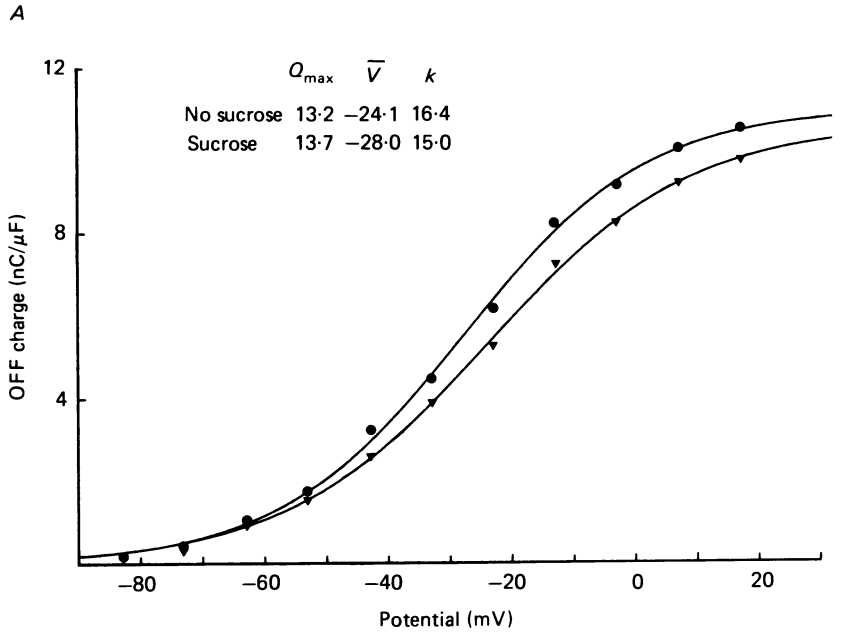

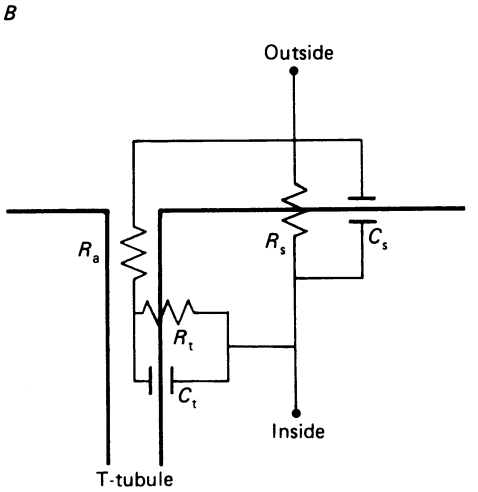

Fig. 8. *A*, best-fit Boltzmann curves for data from the same fibre sequentially exposed to solution E_1 (no sucrose) (▼)) and solution E_2 (80 mM-sucrose (●)). The Boltzmann parameters for each curve are indicated. Sucrose shifted the charge *vs.* potential relation to more negative potentials as well as increasing its steepness (lower k) and the maximum charge (Q_{max}). *B*, a circuit superimposed on a schematic diagram of a section of a muscle fibre, illustrating a simple lumped model of the resistive and capacitive elements of the surface membrane (R_s, C_s) and the transverse tubular membrane (R_t, C_t) as well as the resistance (R_a) at the mouth of and along the tubular system.

Effect of sucrose on the charge vs. potential relation

The effect of sucrose on the relation between charge movement and membrane potential is illustrated in Fig. 8*A*. The data obtained before and after the addition of 80 mM-sucrose to the external solution were fitted by Boltzmann curves (eqn. (6)). The addition of sucrose produced a steeper curve which was shifted to more negative potentials and had a slightly (4 %) higher maximum. An increase of 5 % in the linear capacitance was also observed. These effects of sucrose addition, together with the increase in the speed of both the linear capacitive charging and the asymmetric charge movement, can be adequately explained with reference to a simple lumped model of a section of a muscle fibre (Fig. 8*B*) (see Discussion).

DISCUSSION

Asymmetric charge movement in mammalian muscle has previously been investigated in the rat using micro-electrodes with contractions blocked by hypertonic sucrose solutions (Hollingworth & Marshall, 1981; Simon & Beam 1985*a*, *b*) or by tetracaine (Dulhunty & Gage, 1983). The use of the Vaseline-gap technique in this study allowed the quantification of charge movement in contracting mammalian fibres and enabled the examination of the effects of hypertonic sucrose solutions (and tetracaine in the following paper). Furthermore, it has been possible to relate the charging of the T-system and movement of asymmetric charge, and hence show that most of the asymmetric charge movement occurs in the T-system.

Comparison with previous results

As asymmetric charge movement can be inactivated by prolonged depolarization (Chandler *et al.* 1976*b*), and linear capacitive current cannot, any contribution of the membrane under the EA and AB seals (Fig. 1) (where the potential is depolarized relative to pool A), will result in an underestimation of the normalized charge movement. Horowicz & Schneider (1981*a*) used both the single Vaseline-gap and micro-electrode techniques simultaneously with frog muscle fibres and found that the gap technique indicated about 14 % less charge than did the micro-electrodes. They suggested that the difference may be attributable to the contribution of membrane under the single seal. Though there are a number of differences between single-gap technique and that used here, the question arises as to whether a similar effect underlies the difference between the mean value of Q_{max} in fast-twitch sternomastoid fibres obtained in this study (15·2 nC/μF) and that found in rat fast-twitch muscles with micro-electrodes (48·9, 23·4, 28·3 nC/μF: Hollingworth & Marshall, 1981; Dulhunty & Gage, 1983; Simon & Beam, 1985*a*). This is almost certainly not the case as the rat e.d.l. fibre examined in this study had a considerably higher Q_{max} (24·1 nC/μF) than any of the rabbit sternomastoid fibres, and this value was very close to that found in micro-electrode experiments using the same muscle type, step protocol and similar solutions (23·4 nC/μF, Dulhunty & Gage, 1983). Hence, the smaller amount of charge found in sternomastoid fibres is probably not due to the use of the Vaseline-gap technique. The difference in the charge between rabbit sternomastoid and rat e.d.l. muscles is probably not due to a species difference, but

to a difference between the two types of fast-twitch muscle. The difference in the values might merely be a reflection of the charge movement being normalized by the fibre capacitance. White sternomastoid fibres have capacitances (rat, 13·5 μF/cm^2; rabbit, 13·8 μF/cm^2) that are 70–100% greater than those of e.d.l. fibres (rat, 7·9 μF/cm^2; 6·6 μF/cm^2) (Dulhunty *et al.* 1984; A. F. Dulhunty, P. W. Gage & G. D. Lamb, unpublished observations). Consequently, the two type of fast-twitch muscle possess a similar amount of asymmetric charge per unit of visualized surface area (about 0·2 μC/cm^2).

Charge movement near threshold

The charge movement data from mammalian muscle reported in this paper bear many similarities to results from amphibian muscle. In the rabbit sternomastoid fibres, the amount of charge moved at contraction threshold was roughly half of the maximum charge (q_{th} = 8·5, Q_{max} = 16·3 nC/μF), which is similar to results reported for frog muscle by Horowicz & Schneider (1981*a*,*b*) (q_{th} = 11·5, Q_{max} = 26·7 nC/μF). Horowicz & Schneider (1981*a*,*b*) used a Vaseline-gap technique and, on finding that q_{th} was higher than that in intact fibres (Adrian, Chandler & Rakowski, 1976; Huang, 1981), proposed that the difference may have resulted from the solutions they used to bathe the cut fibres. Similarly, the cut-fibre technique used in this study may have influenced the potential and charge thresholds found (see Lamb, 1986).

Close examination of the time course of charge movement in rabbit muscle (Figs. 4 and 5) revealed, under some conditions, the presence of a small hump associated with the ON charge. As reported for amphibian muscle, this hump is evident near the threshold potential and as the size of the depolarizing step is increased, it occurs at progressively earlier times until it merges with the main peak of the ON charge. Because of similarities to amphibian muscle it seems appropriate to denote the hump in mammalian charge movement, q_γ. The q_γ component was less apparent in this study than in studies with amphibian muscle, though this may be due to the different temperatures used (22 and 2 °C). Alternatively, considering the prominent q_γ component seen in the largest fibre in this study (Fig. 5), the structural dimensions of a fibre may affect the relative size of the charge movement components. The data shown in Fig. 5 also suggested that there may not be a fixed relation between the amount of q_γ and that of the main component of charge, q_β. A more thorough study of mammalian fibres showing a prominent q_γ component is needed to investigate the relation properly. A distinct q_γ component could not be identified, in many contracting rabbit fibres, although it may have occurred as a small slow component following the ON charge rather than as a distinct hump; this was supported by the observation that in these fibres the area of the main ON charge peak was unaccountably smaller than that of the OFF charge peak. The occurrence of such a slow component would not be surprising in view of the observation that in frog muscle q_γ near threshold has a very long time course (Adrian & Huang, 1984*a*).

The T-system and asymmetric charge movement

The slower of the two components apparent in the linear capacitive current produced by a step change in potential (Fig. 6) closely reflects the charging of the transverse tubular (T-) system (Hille & Campbell, 1976). Hence the relation between

the charging of the linear capacitance and the speed of charge movement (Fig. 7) strongly suggests that the asymmetric charge is located in the T-system (or beyond). A similar conclusion was reached in a recent micro-electrode study (Simon & Beam, 1985*a*). This conclusion differs from that of Adrian & Huang (1984*b*), who suggested that q_β is located at the fibre surface because only the total charge ($q_\beta + q_\gamma$), and not q_β alone, was greater in larger fibres. However, no such relation between fibre diameter and the total charge moved by a 10 mV step was observed in this study, although this may be the result of errors in the measurement of linear capacitance (see earlier) affecting this type of analysis.

Purely because of the heavier filtering used, it was to be expected that the asymmetric charge would lag behind the linear capacitive transient by about 0·75 ms. Hence the intercept of the best-fit line with the ordinate in Fig. 7 (1·2 ms) indicates that, at 22 °C, the asymmetric charge must have moved very soon (about 0·5 ms) after depolarization of the T-system, which is essential if charge movement, or some subdivision, plays a role in excitation–contraction coupling.

The effects of hypertonic sucrose solutions

The effect of sucrose on (a) the speed of charge movement and (b) the Q *vs.* V relation (Fig. 8*A*) can be understood by consideration of the principal resistive and capacitive elements in a muscle fibre. If a potential difference (p.d.) of magnitude E is imposed at time $t = 0$ between the inside and outside of the cell shown in Fig. 8*B*, then the p.d. across the tubular membrane, V_t, is given by:

$$V_t = E\frac{R_t}{R_t + R_a}\left(1 - e^{\frac{-t}{R_{eq}C_t}}\right), \tag{7}$$

where

$$R_{eq} = \frac{R_a R_t}{R_a + R_t}. \tag{8}$$

In Fig. 8*B* asymmetric charge movement is assumed to be affected by the potential difference across the tubular membrane. If the addition of sucrose to the external solution dilates the transverse tubules or their mouths, whether by osmotic effects or otherwise, a number of events will follow. (1) The resistance, R_a, in series with the tubular membrane will decrease. (2) As a consequence, a larger fraction of any potential difference between the inside of the cell and the external solution, will be seen across the tubular membrane (eqn. 7). (3) This will result in an increase in the apparent linear capacitance. Furthermore, any potential step (smaller than that producing maximum charge movement) will move a larger amount of asymmetric charge than it would in the absence of sucrose, leading to a steepening and negative shift of the charge *vs.* potential relation (Fig. 8*A*). (4) The rate at which a step in potential across the surface membrane appears across the tubular membrane is inversely related to the resistance down the tubule, R_a (eqns. 7 and 8), and consequently addition of sucrose will increase the speed of charging of the tubular capacitance and, hence, the speed of the asymmetric charge movement as well (Fig. 6).

The magnitude of these effects will depend on the values of R_a and R_t. A rough estimate of the relative resistances in the lumped circuit shown in Fig. 8*B* can be

obtained in the following way. Table 2 suggests that the mean tubular capacitance, C_t, was at least 12 μF/cm^2, and the value of the time constant $R_{eq}C_t$ is approximately half of the time taken for 90 % charging of the linear capacitance (Fig. 7), and ranged between 1 and 5 ms. Hence R_{eq} ranged between 80 and 400 Ω cm^2. The total resistance of the parallel current paths R_s and (R_a+R_t) is at least 2·2 kΩ cm^2 (Table 2), so the resistance (R_a+R_t) must be at least as great. Thus if (R_a+R_t) is much lower than R_s, from eqn. (8) the ratio of R_a to R_t is between 1:21 and 1:3·2. Alternatively, if (R_a+R_t) is considerably greater than R_s, say 10 kΩ cm^2, the ratio is between 1:100 and 1:24.

As R_a is probably far smaller than R_t, moderate changes in R_a will cause only relatively small effects on the Q *vs.* V relation and on the measured capacitance, but will still produce considerable changes in the time course of the linear capacitive current.

Thus all the results observed upon the addition of sucrose can be readily explained if it causes a simple dilation of part of the T-system. (The small increase in Q_{max} can be accounted for by a more general distributed model of resistive and capacitive elements in the tubular system, together with charge saturation.) Such swelling of the T-system in hypertonic sucrose solutions has been observed in two morphological studies (Davey & O'Brien, 1978; Franzini-Armstrong, Heuser, Reese, Somlyo & Somlyo, 1978). (Shortening of the T-system, owing to a decrease in fibre diameter, could also contribute to a decrease in R_a.) This simple effect of sucrose provides an explanation for the more negative $\bar{V}$ and smaller k found in previous charge movement experiments using sucrose compared to those without it, in both mammals (Hollingworth & Marshall, 1981; Dulhunty & Gage, 1983; Simon & Beam, 1985*a*,*b*) and amphibia (Adrian & Almers, 1976; Almers & Best, 1976; Chandler *et al.* 1976*a*; Campbell, 1983; Hui, 1983). Similarly, it can account for the slower time course of the potassium tail currents observed in rat skeletal muscle by Duval & Leoty (1980) using a Ringer solution, compared to that seen by Beam & Donaldson (1983) using a hypertonic sucrose solution. The magnitude of the sucrose effects depended on the concentration added; in this study 290 mM-sucrose produced greater effects than 80 mM-sucrose. It also depended on the length of time that the fibres were bathed in particular solutions; fibres were seen to swell slowly in the A pool when surrounded by an 'isotonic' TEABr solution, and this was accompanied by a progressive slowing of the linear capacitance. In summary, it is clear that better potential control of the T-system could be achieved with sucrose in the external solution.

I am grateful to Professor P. W. Gage and to Dr A. F. Dulhunty for their advice throughout this project and their comments on this paper. Dr D. Adams provided invaluable help with building the clamp and with the dissection procedure. I also wish to thank Mr R. Malbon, Mrs E. Elekessy and Dr J. Dawson for programming assistance, Mrs B. McLachlan for technical assistance and Miss J. Livingstone for preparing the manuscript.

REFERENCES

ADRIAN, R. H. & ALMERS, W. (1976). Charge movement in the membrane of striated muscle. *Journal of Physiology* **254**, 339–360.

ADRIAN, R. H., CHANDLER, W. K. & HODGKIN, A. L. (1970). Voltage clamp experiments in striated muscle fibres. *Journal of Physiology* **208**, 607–644.

ADRIAN, R. H., CHANDLER, W. K. & RAKOWSKI, R. F. (1976). Charge movement and mechanical repriming in skeletal muscle. *Journal of Physiology* **254**, 361–388.

ADRIAN, R. H. & HUANG, C. L-H. (1984*a*). Charge movements near the mechanical threshold in skeletal muscle of *Rana temporaria*. *Journal of Physiology* **349**, 483–500.

ADRIAN, R. H. & HUANG, C. L-H. (1984*b*). Experimental analysis of the relationship between charge movement components in skeletal muscle of *Rana temporaria*. *Journal of Physiology* **353**, 419–434.

ADRIAN, R. H. & PERES, A. (1979). Charge movement and membrane capacity in frog muscle. *Journal of Physiology* **289**, 83–97.

ALMERS, W. & BEST, P. M. (1976). Effects of tetracaine on displacement currents and contraction of frog skeletal muscle. *Journal of Physiology* **262**, 583–611.

ALMERS, W., MCCLESKEY, E. W. & PALADE, P. T. (1984). A non-selective cation conductance in frog muscle membrane blocked by micromolar external calcium ions. *Journal of Physiology* **353**, 565–583.

BEAM, K. G. & DONALDSON, P. L. (1983). A quantitative study of potassium channel kinetics in rat skeletal muscle from 1 to 37 °C. *Journal of General Physiology* **81**, 485–512.

CAMPBELL, D. T. (1983). Sodium channel gating currents in frog skeletal muscle. *Journal of General Physiology* **82**, 679–701.

CAMPBELL, D. T. & HAHIN, R. (1983). Functional disruption of the T-system of cut muscle fibres bathed in solutions of normal tonicity. *Biophysical Journal* **41**, 177*a*.

CHANDLER, W. K., RAKOWSKI, R. F. & SCHNEIDER, M. F. (1976*a*). A non-linear voltage dependent charge movement in frog skeletal muscle. *Journal of Physiology* **254**, 245–283.

CHANDLER, W. K., RAKOWSKI, R. F. & SCHNEIDER, M. F. (1976*b*). Effects of glycerol treatment and maintained depolarization on charge movement in skeletal muscle. *Journal of Physiology* **254**, 285–316.

DAVEY, D. F. & O'BRIEN, G. M. (1978). The sarcoplasmic reticulum and T-system of rat extensor digitorum longus muscles exposed to hypertonic solutions. *Australian Journal of Experimental Biology and Medical Science* **56**, 409–419.

DULHUNTY, A. F., CARTER, G. & HINRICHSEN, C. (1984). The membrane capacity of mammalian skeletal muscle fibres. *Journal of Muscle Research and Cell Motility* **5**, 315–332.

DULHUNTY, A. F. & GAGE, P. W. (1983). Asymmetrical charge movement in slow- and fast-twitch mammalian muscle fibres in normal and paraplegic rats. *Journal of Physiology* **341**, 213–231.

DULHUNTY, A. F. & GAGE, P. W. (1985). Excitation–contraction coupling and charge movement in denervated rat extensor digitorum longus and soleus muscles. *Journal of Physiology* **358**, 75–89.

DULHUNTY, A. F., GAGE, P. W. & BARRY, P. H. (1981). Asymmetrical charge movement in normal and glycerol treated toad sartorius fibres. In *Advances in Physiological Science*, vol. **5**, *Molecular and Cellular Aspects of Muscle Function*, ed. VARGA, E., KOVER, A., KOVACS, T. & KOVACS, L. pp. 321–327. Oxford: Pergamon Press.

DUVAL, A. & LEOTY, C. (1978). Ionic currents in mammalian fast twitch skeletal muscle. *Journal of Physiology* **278**, 403–423.

DUVAL, A. & LEOTY, C. (1980). Comparison between the delayed outward current in slow and fast twitch muscle in the rat. *Journal of Physiology* **307**, 43–57.

FRANZINI-ARMSTRONG, C., HEUSER, J. E., REESE, T. S., SOMLYO, A. P. & SOMLYO, A. V. (1978). T-tubule swelling in hypertonic solutions: a freeze substitution study. *Journal of Physiology* **283**, 133–140.

HILLE, B. & CAMPBELL, D. T. (1976). an improved vaseline gap voltage clamp for skeletal muscle fibres. *Journal of General Physiology* **67**, 265–293.

HOLLINGWORTH, S. & MARSHALL, M. W. (1981). A comparative study of charge movements in rat and frog skeletal muscle fibres. *Journal of Physiology* **321**, 583–602.

HOROWICZ, P. & SCHNEIDER, M. F. (1981*a*). Membrane charge movement in contracting and non-contracting skeletal muscle fibres. *Journal of Physiology* **314**, 565–593.

HOROWICZ, P. & SCHNEIDER, M.F. (1981*b*). Membrane charge moved at contraction thresholds in skeletal muscle fibres. *Journal of Physiology* **314**, 595–633.

HUANG, C. L-H. (1981). Effects of local anaesthetics on the relationship between charge movements and contractile thresholds in frog skeletal muscle. *Journal of Physiology* **320**, 381–391.

HUANG, C. L-H. (1982). Pharmacological separation of charge movement components in frog skeletal muscle. *Journal of Physiology* **324**, 375–387.

HUI, C. S. (1983). Pharmacological studies of charge movement in frog skeletal muscle. *Journal of Physiology* **337**, 509–529.

KOVACS, L., RIOS, E. & SCHNEIDER, M. F. (1979). Calcium transients and intramembrane charge movement in skeletal muscle fibres. *Nature* **279**, 391–396.

LAMB, G. D. (1985*a*). The effect of nifedipine on asymmetric charge movement in rabbit muscle. *Proceedings of the Australian Physiological and Pharmacological Society* **16**, 2*P*.

LAMB, G. D. (1985*b*). The components of asymmetric charge movement in rabbit muscle. *Proceedings of the Australian Physiological and Pharmacological Society* **16**, 228*P*.

LAMB, G. D. (1986). Components of charge movement in rabbit skeletal muscle: the effect of tetracaine and nifedipine. *Journal of Physiology* **376**, 85–100.

SCHNEIDER, M. F. & CHANDLER, W. K. (1973). Voltage dependent charge movement in skeletal muscle: a possible step in excitation–contraction coupling. *Nature* **242**, 244–246.

SCHNEIDER, M. F. & CHANDLER, W. K. (1976). Effects of membrane potential on the capacitance of skeletal muscle fibres. *Journal of General Physiology* **67**, 125–163.

SIMON, B. J. & BEAM, K. G. (1985*a*). Slow charge movement in mammalian muscle. *Journal of General Physiology* **85**, 1–19.

SIMON, B. J. & BEAM, K. G. (1985*b*). The influence of transverse tubular delays on the kinetics of charge movement in mammalian skeletal muscle. *Journal of General Physiology* **85**, 21–42.